

Entangled photons from the polariton vacuum in a switchable optical cavity

Adrian Auer* and Guido Burkard

Department of Physics, University of Konstanz, D-78457 Konstanz, Germany

(Received 14 December 2011; revised manuscript received 23 May 2012; published 21 June 2012)

We study theoretically the entanglement of two-photon states in the ground state of the intersubband cavity system, i.e., the so-called polariton vacuum. The system consists of a sequence of doped quantum wells located inside a microcavity and the photons can interact with intersubband excitations inside the quantum wells. Using an explicit solution for the ground state of the system, operated in the ultrastrong-coupling regime, a postselection is introduced, where only certain two-photon states are considered and analyzed for mode entanglement. We find that a fast quench of the coupling creates entangled photons and that the degree of entanglement depends on the absolute values of the in-plane wave vectors of the photons. Maximally entangled states can be generated by choosing the appropriate modes in the postselection.

DOI: [10.1103/PhysRevB.85.235140](https://doi.org/10.1103/PhysRevB.85.235140)

PACS number(s): 73.21.Fg, 03.67.Bg, 71.36.+c, 78.67.De

I. INTRODUCTION

With the advent of quantum information theory,¹ the phenomenon of entanglement not only remained a mysterious feature of quantum mechanics,^{2,3} but became a resource to perform tasks that are not feasible with classical resources. Examples are quantum communication protocols, which make use of entangled states like quantum key distribution,⁴ quantum teleportation,⁵ or superdense coding,⁶ or the realization of a quantum repeater.⁷

Entangled photon states are often used to implement the protocols mentioned above. Today, there exist several different proposals for the production of bipartite entangled photon states, most prominently type-II parametric down-conversion⁸ and biexciton decay in a quantum dot.⁹

The fundamental requirements for such a photon-pair source to be used in quantum information processing are that the states have to possess a sufficient amount of entanglement and that the production of the two photons has to be deterministic and efficient. Determinism means that the release of the photons can be triggered by some external control parameter. Efficiency means that the probability for this event is near unity.

Here, we study the intersubband cavity system, for which the emission of correlated photon pairs was predicted theoretically¹⁰ and can be triggered by modulating the light-matter interaction between microcavity photons and electronic excitations in the quantum wells (QWs). Those intersubband transitions are mainly used in quantum-well infrared photodetectors¹¹ and quantum cascade lasers.^{12–15} Embedded in a microcavity, it is possible to reach a regime of ultrastrong light-matter coupling,^{16–19} in which the vacuum-field Rabi frequency can be of the order of the intersubband transition frequency, and the ground state of the system, i.e., a squeezed vacuum, contains already a nonzero number of photons. Another type of system, which can reach the ultrastrong-coupling regime as well, is superconducting circuits,^{20–22} where the emission of quantum vacuum radiation was just recently demonstrated.²³

In this paper, we analyze the ground state of the intersubband cavity system, i.e., the so-called polariton vacuum, related to two-photon entanglement. We use an explicit expression for the polariton vacuum and, after postselecting certain

photonic states, quantify the mode entanglement between the photon pairs via the concurrence.

II. THE INTERSUBBAND CAVITY SYSTEM

The intersubband cavity system was intensely studied theoretically; see, e.g., Ref. 10. It consists of n_{QW} identical quantum wells embedded inside a semiconductor optical microcavity (Fig. 1). The quantum wells are assumed to be negatively charged with a two-dimensional electron gas (2DEG) with density N_{2DEG} that populates the first subband (Fig. 2). We consider the interaction of intersubband excitations between the two lowest subbands and photons of the fundamental cavity mode.

The ultrastrong-coupling regime, in which the vacuum-field Rabi splitting is of the order of the intersubband transition energy, can be reached due to the large dipole moment¹⁶ of intersubband transitions and the collective coupling to all electrons of the 2DEGs. In this regime, the rotating-wave approximation²⁴ is not valid anymore and the full light-matter interaction Hamiltonian in the Coulomb gauge including the antiresonant terms has the form¹⁰

$$\begin{aligned}
 H = & \sum_{\mathbf{k}} \hbar \omega_c(\mathbf{k}) \left(a_{\mathbf{k}}^\dagger a_{\mathbf{k}} + \frac{1}{2} \right) + \sum_{\mathbf{k}} \hbar \bar{\omega}_{12}(\mathbf{k}) b_{\mathbf{k}}^\dagger b_{\mathbf{k}} \\
 & + \sum_{\mathbf{k}} i \hbar \Omega_R(\mathbf{k}) (a_{\mathbf{k}}^\dagger + a_{-\mathbf{k}}) (b_{\mathbf{k}} - b_{-\mathbf{k}}^\dagger) \\
 & + \sum_{\mathbf{k}} \hbar D(\mathbf{k}) (a_{\mathbf{k}}^\dagger + a_{-\mathbf{k}}) (a_{-\mathbf{k}}^\dagger + a_{\mathbf{k}}). \quad (1)
 \end{aligned}$$

The operator $a_{\mathbf{k}}^{(\dagger)}$ annihilates (creates) a cavity photon with in-plane wave vector $\mathbf{k} = (k_x, k_y)$ and transverse-magnetic (TM) polarization, while the operator $b_{\mathbf{k}}^{(\dagger)}$ annihilates (creates) an electronic intersubband excitation. Photon polarizations other than TM are excluded due to the selection rule for intersubband transitions:¹¹ since the dipole moment is oriented along the growth (z) direction, the exciting radiation must have a finite electric-field component in the z direction. As shown in Fig. 1, the magnetic field for TM-polarized light is perpendicular to the plane of incidence, whereas the electric field has a finite z component if the wave vector encloses a finite angle θ with the normal to the cavity mirror. Our analysis also applies to

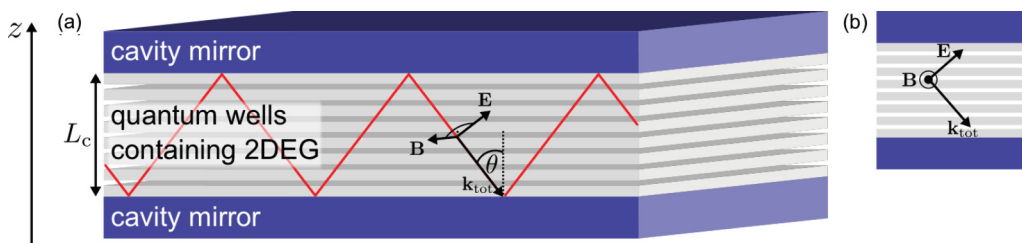


FIG. 1. (Color online) (a) The system under consideration: A sequence of doped QWs (gray) inside a microcavity of length L_c (cavity mirrors in blue) form the intersubband cavity system. The light-matter interaction in such a system depends on the propagation angle θ of the cavity photons. The transverse-magnetic polarization is indicated by the electric and magnetic field vectors. The electric field \mathbf{E} lies in the plane of incidence and the magnetic field \mathbf{B} is perpendicular to it, and both are perpendicular to the photon wave vector \mathbf{k}_{tot} . (b) The plane of incidence to better demonstrate the TM polarization of the photons.

the case where the polarization is not purely TM because only the TM-polarized part of the radiation couples to intersubband transitions.

The dispersion of the fundamental cavity mode $\omega_c(k)$ is given by

$$\omega_c(k) = \frac{c}{\sqrt{\varepsilon}} \sqrt{k^2 + k_z^2}, \quad (2)$$

where c is the speed of light, ε is the dielectric constant of the material used as the cavity spacer, and the quantization of k_z can depend in a complicated way on the boundary conditions. In the following, $k = |\mathbf{k}|$ is the length of the in-plane wave vector.

The ultrastrong-coupling regime can only be reached if the electron density N_{2DEG} is sufficiently high, i.e., about 10^{12} cm^{-2} [see Eq. (6) below]. For such high densities, the renormalization of the intersubband energy,

$$\bar{\omega}_{12}^2(k) = \omega_{12}^2(1 + \delta(k)), \quad (3)$$

known as the depolarization shift,¹¹ can in general not be neglected. Equation (3) can be derived by adding a Coulomb-interaction term to the single-particle Hamiltonian, i.e., Eq. (1)

with $\bar{\omega}_{12}(k)$ replaced by ω_{12} .¹⁰ The depolarization shift $\delta(k)$ is found to be^{25,26}

$$\delta(k) = \frac{N_{\text{2DEG}} e^2 I(k)}{\varepsilon_0 \varepsilon \omega_{12} k}, \quad (4)$$

where e is the elementary charge, ε_0 is the vacuum permittivity, and ω_{12} is the intersubband frequency difference, which in the absence of interactions determines the absorption maximum. The function $I(k)$ originates from the two-dimensional Coulomb integral,

$$I(k) = \int dz dz' \varphi_1(z) \varphi_2(z) \varphi_2(z') \varphi_1(z') e^{-k|z-z'|}, \quad (5)$$

where $\varphi_{1,2}(z)$ are the z -dependent parts of the (real) QW wave functions of subbands 1 and 2, respectively. A Bogoliubov transformation²⁷ of the operators describing single-particle excitations in the QWs finally leads to the Hamiltonian (1) with the renormalized intersubband transition energy $\bar{\omega}_{12}(k)$ as given in Eq. (3). The depolarization shift describes a change in the spatial charge distribution in the 2DEG (plasmonic excitation) due to the excitation of a single electron from subband 1 to 2.

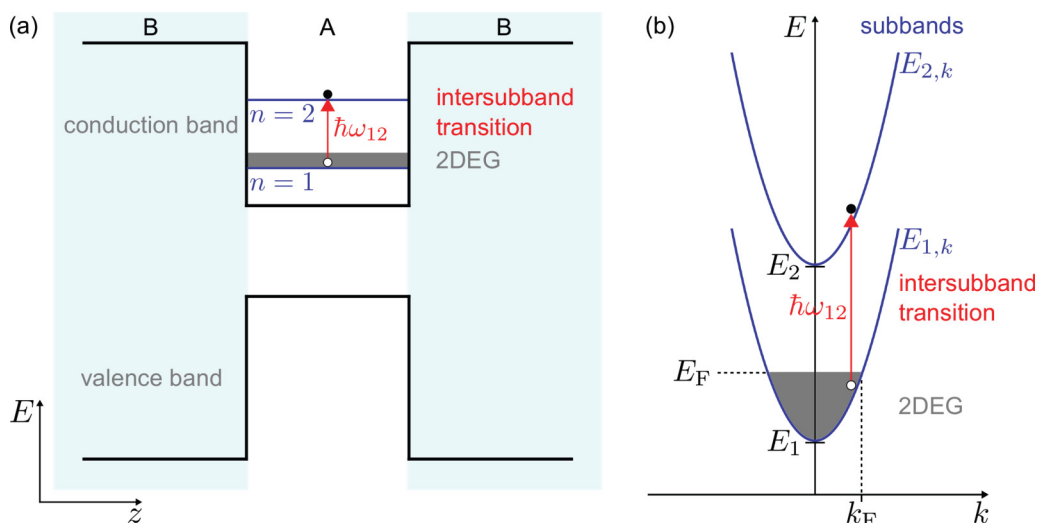


FIG. 2. (Color online) Subband energy structure of a quantum well (QW) formed in a semiconductor heterostructure. (a) In real space, along the growth direction z of the structure, the semiconductors forming the QW are denoted as A and B. The QW contains a two-dimensional electron gas (2DEG). Here, we study intersubband transitions between the first two subbands, $n = 1$ and $n = 2$, with transition energy $\hbar\omega_{12}$. (b) The same situation in k space, where the 2DEG populates states up to the Fermi energy E_F , with a corresponding wave vector k_F .

Hence, the $b_k^{(\dagger)}$ in Eq. (1) are plasmonic operators describing collective electronic excitations and are obtained by a Bogoliubov transformation of the single-particle operators.²⁷ They fulfill Bose commutation relations $[b_k, b_k^\dagger] \simeq \delta_{k,k}$ in the weak excitation regime, i.e., when the number of intersubband excitations is much less than the number of electrons forming the 2DEG.^{10,28}

The vacuum Rabi frequency $\Omega_R(k)$ for the intersubband cavity system is given by^{10,29}

$$\Omega_R(k) = \left[\frac{e^2 N_{2\text{DEG}} n_{\text{QW}}^{\text{eff}} f_{12} \bar{\omega}_{12}(k)}{2\epsilon_0 \epsilon m^* L_c^{\text{eff}} \omega_c(k)} \sin^2 \theta(k) \right]^{\frac{1}{2}}. \quad (6)$$

Here, $n_{\text{QW}}^{\text{eff}}$ is an effective number of embedded quantum wells since not all quantum wells are equally coupled to the photon field, L_c^{eff} denotes an effective cavity thickness that depends on the type of cavity mirrors, and f_{12} is the oscillator strength of the subband transition. For a deep rectangular well, $f_{12} \simeq 1$.^{10,11} Finally, $\theta(k)$ is the propagation angle of a cavity photon: $\sin \theta(k) = k / \sqrt{k^2 + k_z^2}$. The dispersive coupling parameter $D(k)$ can be approximated by $D(k) \simeq \Omega_R^2(k) / \bar{\omega}_{12}(k)$, which is valid for deep rectangular wells and exact for parabolic well potentials.^{10,19}

The Hamiltonian (1) can be diagonalized with an extended Bogoliubov transformation,³⁰ also known as Hopfield transformation,³¹ where new bosonic operators

$$p_{j,k} = w_j(k) a_k + x_j(k) b_k + y_j(k) a_{-k}^\dagger + z_j(k) b_{-k}^\dagger \quad (7)$$

are introduced that describe a quasiparticle called intersubband cavity polariton,³² and j indicates whether it belongs to the lower ($j = \text{LP}$) or upper ($j = \text{UP}$) polariton branch. The wave vectors \mathbf{k} are still meant to be in-plane. By an appropriate choice of the Hopfield coefficients $w_j(k)$, $x_j(k)$, $y_j(k)$, and $z_j(k)$, which are already taken to depend only on k , the Hamiltonian becomes diagonal,

$$H = E_G + \sum_{j \in \{\text{LP}, \text{UP}\}} \sum_{\mathbf{k}} \hbar \omega_j(k) p_{j,k}^\dagger p_{j,k}. \quad (8)$$

Here, E_G denotes the ground-state energy. The resulting lower and upper polariton dispersions are shown in Fig. 3. Here, as well as for all further quantitative results, we assume GaAs/AlGaAs quantum wells, which have been commonly used experimentally.^{16,32–34} Hence, the material-dependent parameters are $m^* = 0.067m_0$ and $\epsilon = 10$. Furthermore, the number of embedded quantum wells n_{QW} , the length of the microcavity L_c , and the subband level spacing ω_{12} , which is determined by the quantum-well depth and thickness, can be adjusted during the manufacturing process. The density of the two-dimensional electron gas can be varied experimentally. To obtain the results of Fig. 3, we chose $n_{\text{QW}}^{\text{eff}} = 50$, $L_c^{\text{eff}} = 2 \mu\text{m}$, $\hbar\omega_{12} = 113 \text{ meV}$, and $N_{2\text{DEG}} = 10^{12} \text{ cm}^{-2}$ as one particular set of experimentally reasonable values of the parameters mentioned above, on the basis of the experimental work done in Ref. 16. The ultrastrong-coupling regime has also been reached using zero-dimensional (0D) cavities operating in the THz regime.¹⁸ However, 0D cavities are not suited for our entanglement generation scheme because only one of their modes couples to the QW transition, whereas our proposed scheme for mode entanglement

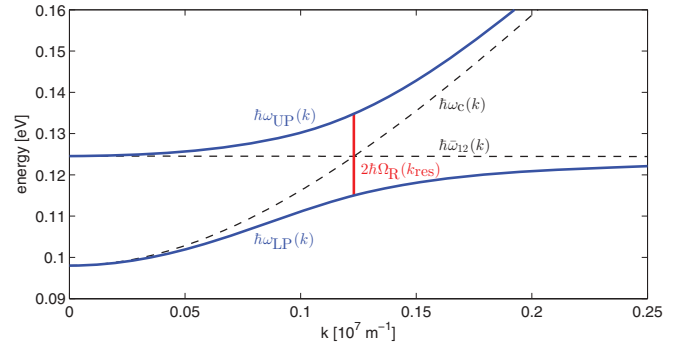


FIG. 3. (Color online) The polariton energy dispersions $\hbar\omega_{\text{LP}}(k)$ and $\hbar\omega_{\text{UP}}(k)$ as a function of the absolute value of the in-plane wave vector k . Here, $n_{\text{QW}}^{\text{eff}} = 50$ GaAs/AlGaAs ($\epsilon = 10.0$, $m^* = 0.067m_0$) QWs are assumed to be located inside a cavity of length $L_c^{\text{eff}} = 2 \mu\text{m}$ and doped with a two-dimensional electron gas density of $N_{2\text{DEG}} = 10^{12} \text{ cm}^{-2}$. The plot shows the anticrossing region where the dotted lines are the bare cavity photon dispersion $\hbar\omega_c(k)$ and the intersubband transition energy $\hbar\omega_{12}(k)$. The vacuum-field Rabi splitting is $2\hbar\Omega_R(k_{\text{res}})$. This plot takes into account the depolarization shift, $\bar{\omega}_{12}(k) = \omega_{12}\sqrt{1 + \delta(k)}$, with $\hbar\omega_{12} = 113 \text{ meV}$ (Ref. 16).

(see below) requires the coupling to several distinct modes simultaneously.

The ground state of the intersubband cavity system, operating in the ultrastrong-coupling regime, is not the ordinary vacuum $|0\rangle$, in which there are no cavity photons and no intersubband excitations present,

$$a_{\mathbf{k}}|0\rangle = b_{\mathbf{k}}|0\rangle = 0, \quad (9)$$

but a state $|G\rangle$ that exhibits no intersubband cavity polaritons,

$$p_{j,k}|G\rangle = 0, \quad j \in \{\text{LP}, \text{UP}\}. \quad (10)$$

Without knowing the explicit form of $|G\rangle$, one can show that the ground state has some peculiar properties in the ultrastrong-coupling regime that were worked out in Ref. 10, whereof the essential ones are that it contains a finite number of photons,

$$\langle G|a_{\mathbf{k}}^\dagger a_{\mathbf{k}}|G\rangle = |y_{\text{LP}}(k)|^2 + |y_{\text{UP}}(k)|^2, \quad (11)$$

and photons with opposite in-plane wave vectors \mathbf{k} and $-\mathbf{k}$ are correlated,

$$\langle G|a_{\mathbf{k}} a_{-\mathbf{k}}|G\rangle = -w_{\text{LP}}^*(k) y_{\text{LP}}(k) - w_{\text{UP}}^*(k) y_{\text{UP}}(k). \quad (12)$$

One can see that only if the light-matter interaction is so strong that the Hopfield coefficients $y_{\text{LP}}(k)$ and $y_{\text{UP}}(k)$ are reasonably large, that is, $|y_j(k)|^2 \sim 0.1$ [i.e., when the antiresonant terms of the light-matter interaction Hamiltonian cannot be neglected and therefore the extended Bogoliubov transformation (7) is necessary], then the ground state $|G\rangle$ differs significantly from the vacuum state $|0\rangle$.

The idea is now that the correlations (12) can lead to entanglement of two photons propagating in opposite directions. These photons are, however, virtual excitations, but it is conjectured^{10,35,36} that they can be released by a nonadiabatic switch-off (quench) of the vacuum Rabi frequency $\Omega_R(k)$. An experimental approach to this scenario is an ultrafast change of the density $N_{2\text{DEG}}$ of two-dimensional electron gas.^{16,33,34} One mechanism to achieve a modulation of the

parameter $N_{2\text{DEG}}$ is a gate voltage, which can lead to the depletion of the QWs.³³ The rapidity is restricted by the capacitance of the gates, however. Another implementation uses two asymmetrically coupled QWs, in which one QW can be charged by electron tunneling and this process can happen on the picosecond time scale or faster.³⁴ A promising idea to achieve an ultrafast coupling modulation is an all-optical control scheme,¹⁶ in which electrons from the valence band are resonantly excited to the first subband by a femtosecond laser pulse. In this manner, it could be demonstrated experimentally that the coupling between the cavity photon field and the intersubband transitions in the quantum wells can be switched on in a time shorter than a cycle of light in the microcavity. Since then, further progress has been made in the field of ultrafast switching the light-matter interaction strength, experimentally^{37,38} and theoretically.³⁹ In Refs. 35 and 36, the spectrum of the radiation exiting the cavity was derived in more detailed calculations, when a time-dependent coupling $\Omega_R(k,t)$ is predominant in the system and it is predicted that the vacuum radiation rises above the blackbody radiation.

III. EXACT GROUND STATE

A pioneering calculation of the polariton ground state of a bulk dielectric was given by Quattropani *et al.*³¹ The solution is given by independent photon and polarization states. Since the Hamiltonian of the intersubband cavity system is similar to the one in Ref. 31, we use their treatment to determine the explicit form of the polariton vacuum $|G\rangle$ being the ground state of the Hamiltonian (1) of the intersubband cavity system. The difference is just that the sums in (1) cover all in-plane wave vectors.

The ansatz for the polariton vacuum $|G\rangle$ is

$$|G\rangle = \frac{1}{N} e^{\frac{i}{2} \sum_k [G(k)(a_k^\dagger a_{-k}^\dagger + b_k^\dagger b_{-k}^\dagger) + F(k)(a_k^\dagger b_{-k}^\dagger + b_k^\dagger a_{-k}^\dagger)]} |0\rangle. \quad (13)$$

N is a normalization constant and the expansion coefficients $G(k)$ and $F(k)$ have to be determined in order to satisfy the definition of the polariton vacuum (10):

$$p_{j,k}|G\rangle = 0, \quad j \in \{\text{LP}, \text{UP}\}.$$

We anticipate that the functions $G(k)$ and $F(k)$ will only depend on the absolute value of the in-plane wave vector k . After some algebra using commutation relations, which is explicitly given in Ref. 31, the action of a_k and b_k on $|G\rangle$ is, e.g.,

$$a_k|G\rangle = (G(k)a_{-k}^\dagger + F(k)b_{-k}^\dagger)|G\rangle, \quad (14)$$

$$b_k|G\rangle = (G(k)b_{-k}^\dagger + F(k)a_{-k}^\dagger)|G\rangle. \quad (15)$$

By inserting (14) and (15) into the definitions (7) and (10), one obtains a system of equations for the coefficients $G(k)$ and $F(k)$,

$$w_j(k)G(k) + x_j(k)F(k) + y_j(k) = 0, \quad (16)$$

$$w_j(k)F(k) + x_j(k)G(k) + z_j(k) = 0, \quad (17)$$

which has the solutions

$$G(k) = \frac{x_j(k)z_j(k) - w_j(k)y_j(k)}{w_j^2(k) - x_j^2(k)}, \quad (18)$$

$$F(k) = \frac{x_j(k)y_j(k) - w_j(k)z_j(k)}{w_j^2(k) - x_j^2(k)}. \quad (19)$$

This can be fulfilled simultaneously by the Hopfield coefficients of the lower and upper polariton, which can be seen from the following relations:^{30,31}

$$\begin{aligned} w_{\text{LP}}(k) &= x_{\text{UP}}(k), & x_{\text{LP}}(k) &= w_{\text{UP}}(k), \\ y_{\text{LP}}(k) &= z_{\text{UP}}(k), & z_{\text{LP}}(k) &= y_{\text{UP}}(k). \end{aligned} \quad (20)$$

By inserting the explicit expressions of the Hopfield coefficients, the expansion coefficients can be rewritten as³¹

$$G(k) = \frac{\bar{\omega}_{12}(k) + \omega_c(k) - \omega_{\text{LP}}(k) - \omega_{\text{UP}}(k)}{\bar{\omega}_{12}(k) - \omega_c(k) - \omega_{\text{LP}}(k) - \omega_{\text{UP}}(k)}, \quad (21)$$

$$F(k) = -i \frac{\bar{\omega}_{12}(k)}{\Omega_R(k)} G(k). \quad (22)$$

Finally, the polariton vacuum $|G\rangle$ is calculated to be

$$|G\rangle = \frac{1}{N} e^{\frac{i}{2} \sum_k G(k)(a_k^\dagger a_{-k}^\dagger + b_k^\dagger b_{-k}^\dagger - 2i \frac{\bar{\omega}_{12}(k)}{\Omega_R(k)} a_k^\dagger b_{-k}^\dagger)} |0\rangle \quad (23)$$

because the last two terms in the exponential can be combined, and with the normalization N given by

$$N = \prod_k (|w_{\text{LP}}(k)|^2 + |x_{\text{LP}}(k)|^2)^{\frac{1}{2}}. \quad (24)$$

The dependence of $G(k)$ and $|F(k)|$ on k is plotted in Fig. 4. One can see that $|F(k)|$ is about one order of magnitude larger than $G(k)$ and

$$G(k) \approx |F(k)|^2 \ll 1, \quad (25)$$

in which this was checked for a wide range of experimentally acceptable values of the parameters n_{QW} , L_c , ω_{12} , and $N_{2\text{DEG}}$. Therefore, the polariton vacuum state $|G\rangle$ will be expanded in a Taylor series to the second order in these coefficients as an approximation.

If the light-matter interaction is turned off [$\Omega_R(k) = 0$], then $G(k)$ and $F(k)$ are zero, so the ground state would be the ordinary vacuum $|0\rangle$, as expected.

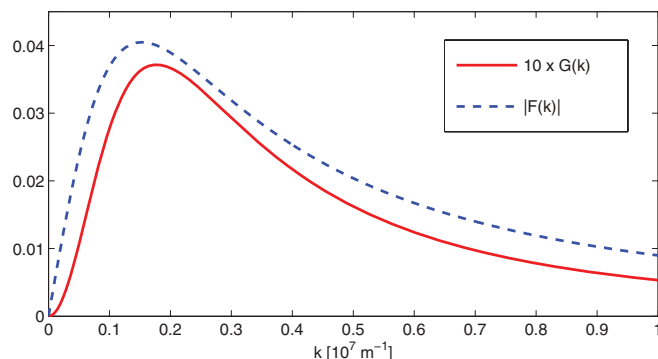


FIG. 4. (Color online) The absolute values of the expansion coefficients $G(k)$ and $|F(k)|$ as a function of the length k of the in-plane wave vector. Parameter values: $\varepsilon = 10$, $m^* = 0.067m_0$, $n_{\text{QW}}^{\text{eff}} = 50$, $L_c^{\text{eff}} = 2 \mu\text{m}$, $\hbar\omega_{12} = 113 \text{ meV}$, $N_{2\text{DEG}} = 10^{12} \text{ cm}^{-2}$. Here, the depolarization shift is taken into account.

IV. PHOTON ENTANGLEMENT

An entangled pure state $|\psi\rangle$, describing two subsystems A and B, is defined by the impossibility of preparing it as a product state, $|\psi\rangle = |\phi\rangle_A \otimes |\nu\rangle_B$, in which $|\phi\rangle_A$ and $|\nu\rangle_B$ are states solely of the subsystems A and B, respectively.⁴⁰ Furthermore, a mixed state ρ is entangled if it cannot be written as a convex combination, $\rho = \sum_{i=1}^n p_i \rho_i^A \otimes \rho_i^B$, where $0 \leq p_i \leq 1$, and again ρ_i^A and ρ_i^B describe the subsystems and n is bounded by the dimensions of the subsystems.⁴⁰

Now, a lot of protocols in quantum information processing⁴⁻⁷ require the distribution of one of the so-called Bell states,⁴¹

$$|\Phi^\pm\rangle = \frac{1}{\sqrt{2}}(|0\rangle_A \otimes |0\rangle_B \pm |1\rangle_A \otimes |1\rangle_B), \quad (26)$$

$$|\Psi^\pm\rangle = \frac{1}{\sqrt{2}}(|0\rangle_A \otimes |1\rangle_B \pm |1\rangle_A \otimes |0\rangle_B), \quad (27)$$

which are maximally entangled states of a system consisting of two qubits with basis $\{|0\rangle, |1\rangle\}$. The term maximally entangled stems from the fact that by using only local operations and classical communication (LOCC), every other pure or mixed state can be created from the Bell states.⁴² But, it is not possible to increase the degree of entanglement by LOCC, since they only lead to classical correlations. Hence, the Bell states must be maximally entangled.

The reliability of a quantum communication protocol depends on the entanglement of the distributed two-qubit state. Thus, for practical reasons, it is important to quantify the amount of entanglement a state has. For pure bipartite states, the entanglement measure is the von Neumann entropy of one of the subsystems.⁴³ (It does not matter which subsystem is chosen, since the von Neumann entropies are equal.) The problem arises when dealing with mixed states. It is still an ongoing challenge to characterize the entanglement of mixed bipartite states, not to mention multipartite systems. However, in the case of a two-qubit system, the entanglement is fully specified and can be quantified by the so-called concurrence^{44,45} (see Sec. IV C).

As seen in the previous section, the intersubband cavity system contains a finite number of photons if it is in the ultrastrong-coupling regime. One possibility of a photon pair in the ground state $|G\rangle$ to be entangled will be studied below. After specifying the type of entanglement, it is quantified by the above-mentioned concurrence.

A. Mode entanglement

We first define the type of photon entanglement. Since the transverse-magnetic polarization of the interacting photons is fixed by the selection rule for intersubband transitions,¹¹ polarization entanglement as achieved with parametric down-conversion or the biexciton decay is out of the question. But there exist anomalous correlations between photons with opposite in-plane momentum (12),

$$\langle G|a_{ka-k}|G\rangle = -w_{\text{LP}}^*(k)y_{\text{LP}}(k) - w_{\text{UP}}^*(k)y_{\text{UP}}(k).$$

Our idea is to test the photonic states in $|G\rangle$ for mode or frequency entanglement.⁴¹

In the following, we limit the treatment to only one direction, since the correlations (12) occur only for photons

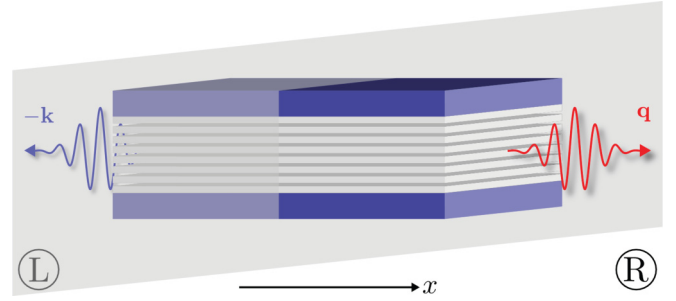


FIG. 5. (Color online) Two photons with different frequencies (colors) leaving the cavity in opposite directions. The two subsystems, left (L) and right (R), are defined via the sign of k_x . Since there is a difference in frequency, the photons have different in-plane wave vectors.

with exactly opposite in-plane wave vectors. This direction is chosen to be the x direction. This is shown schematically in Fig. 5. Photons with a negative (positive) x component of the wave vector belong to subsystem L (R), for left (right).

$|G\rangle$ itself is a vector from a Hilbert space \mathcal{H} , which has a tensor product structure $\mathcal{H} = \mathcal{F}^a \otimes \mathcal{F}^b$, where \mathcal{F}^a and \mathcal{F}^b denote the Fock spaces of the photons and intersubband excitations, respectively. The situation depicted in Fig. 5 is described by vectors in a subspace $\mathcal{H}_{\text{LR}} \subset \mathcal{H}$, which is itself a tensor product of \mathcal{H}_{L} and \mathcal{H}_{R} , the Hilbert spaces of the subsystems L and R, $\mathcal{H}_{\text{LR}} = \mathcal{H}_{\text{L}} \otimes \mathcal{H}_{\text{R}}$. Since $|G\rangle$ contains states from outside \mathcal{H}_{LR} , we project onto \mathcal{H}_{LR} with an appropriate projection operator, which will be described in the following and could be realized experimentally by a postselective measurement.

B. Postselection

The postselection needs to fulfill the following requirements: first, we only allow for states in which two photons with opposite in-plane wave vectors appear. In addition, the postselection is even more restrictive in terms of allowed modes. We only consider two different modes in each subsystem L and R, respectively, that have, however, the same absolute value of the in-plane wave vector. That is, we choose k and q , with $k \neq q$, and consider the modes $\mathbf{k} = (k, 0)$ and $-\mathbf{k} = (-k, 0)$ and accordingly $\mathbf{q} = (q, 0)$ and $-\mathbf{q} = (-q, 0)$, where all wave vectors point along the x direction. So the basis states of \mathcal{H}_{L} are

$$|\mathbf{k}\rangle_{\text{L}} = a_{-\mathbf{k}}^\dagger |0\rangle_a, \quad (28)$$

$$|\mathbf{q}\rangle_{\text{L}} = a_{-\mathbf{q}}^\dagger |0\rangle_a, \quad (29)$$

where $|0\rangle_a$ is the photon vacuum. The basis of \mathcal{H}_{R} is

$$|\mathbf{k}\rangle_{\text{R}} = a_{\mathbf{k}}^\dagger |0\rangle_a, \quad (30)$$

$$|\mathbf{q}\rangle_{\text{R}} = a_{\mathbf{q}}^\dagger |0\rangle_a. \quad (31)$$

Hence, one possible product basis of \mathcal{H}_{LR} is

$$\begin{aligned} &|\mathbf{k}\rangle_{\text{L}} \otimes |\mathbf{k}\rangle_{\text{R}}, \quad |\mathbf{k}\rangle_{\text{L}} \otimes |\mathbf{q}\rangle_{\text{R}}, \\ &|\mathbf{q}\rangle_{\text{L}} \otimes |\mathbf{k}\rangle_{\text{R}}, \quad |\mathbf{q}\rangle_{\text{L}} \otimes |\mathbf{q}\rangle_{\text{R}}. \end{aligned} \quad (32)$$

For all further calculations, the polariton vacuum $|G\rangle$ is expanded to the second order in the small expansion coefficient $G(k)$,

$$\begin{aligned} |G\rangle &= \frac{1}{N} e^{\frac{1}{2} \sum_k G(k) (a_k^\dagger a_{-k}^\dagger + b_k^\dagger b_{-k}^\dagger - 2i \frac{\tilde{\omega}_{12}(k)}{\Omega_R(k)} a_k^\dagger b_{-k}^\dagger)} |0\rangle \\ &\approx \frac{1}{\tilde{N}} \left[1 + \frac{1}{2} \sum_k G(k) \mathcal{T}_k^\dagger + \frac{1}{8} \left(\sum_k G(k) \mathcal{T}_k^\dagger \right)^2 \right] |0\rangle \\ &\equiv |G^{(2)}\rangle, \end{aligned} \quad (33)$$

where \tilde{N} is a new normalization constant to preserve $\langle G^{(2)} | G^{(2)} \rangle = 1$, and the operator \mathcal{T}_k^\dagger is

$$\mathcal{T}_k^\dagger = a_k^\dagger a_{-k}^\dagger + b_k^\dagger b_{-k}^\dagger - 2i \frac{\tilde{\omega}_{12}(k)}{\Omega_R(k)} a_k^\dagger b_{-k}^\dagger. \quad (34)$$

Thus, the two-photon states with opposite in-plane wave vector, i.e., the states that fulfill the postselection requirements, in linear order are

$$a_k^\dagger a_{-k}^\dagger |0\rangle_a = |\mathbf{k}\rangle_L |\mathbf{k}\rangle_R, \quad (35)$$

$$a_q^\dagger a_{-q}^\dagger |0\rangle_a = |\mathbf{q}\rangle_L |\mathbf{q}\rangle_R, \quad (36)$$

and in second order are

$$a_k^\dagger a_{-k}^\dagger b_k^\dagger b_{-k}^\dagger |0\rangle = |\mathbf{k}\rangle_L |\mathbf{k}\rangle_R \otimes b_k^\dagger b_{-k}^\dagger |0\rangle_b, \quad (37)$$

$$a_q^\dagger a_{-q}^\dagger b_k^\dagger b_{-k}^\dagger |0\rangle = |\mathbf{q}\rangle_L |\mathbf{q}\rangle_R \otimes b_k^\dagger b_{-k}^\dagger |0\rangle_b, \quad (38)$$

$$a_k^\dagger a_{-q}^\dagger b_{-k}^\dagger b_q^\dagger |0\rangle = |\mathbf{q}\rangle_L |\mathbf{k}\rangle_R \otimes b_{-k}^\dagger b_q^\dagger |0\rangle_b, \quad (39)$$

$$a_q^\dagger a_{-k}^\dagger b_{-q}^\dagger b_k^\dagger |0\rangle = |\mathbf{k}\rangle_L |\mathbf{q}\rangle_R \otimes b_{-q}^\dagger b_k^\dagger |0\rangle_b. \quad (40)$$

Here, the explicit expression of the tensor product $|0\rangle = |0\rangle_a \otimes |0\rangle_b$ of the individual vacuum states for photons and intersubband excitations is used and \mathbf{k}' can be an arbitrary in-plane wave vector.

We carry out the postselection by projecting onto these states with a projection operator \mathcal{P}_{LR} ,

$$|\psi_{\text{LR}}\rangle = \frac{\tilde{N}}{N_{\text{LR}}} \mathcal{P}_{\text{LR}} |G^{(2)}\rangle, \quad (41)$$

with N_{LR} being a necessary normalization constant, since the operation is a projection. As an intermediate result, we obtain the pure state $|\psi_{\text{LR}}\rangle$ in which all of the two-photon states fulfilling the conditions of the postselection are extracted. We give an explicit expression for $|\psi_{\text{LR}}\rangle$ in Appendix A.

As we will see below, the reduced density matrix ρ^a of the photonic system is needed for the calculation of the entanglement. We compute ρ^a by tracing out the intersubband excitations,

$$\begin{aligned} \rho^a &= \text{Tr}_b |\psi_{\text{LR}}\rangle \langle \psi_{\text{LR}}| \\ &= \frac{1}{N_{\text{LR}}^2} \begin{pmatrix} Z(k) & 0 & 0 & Y(k,q) \\ 0 & X(k,q) & 0 & 0 \\ 0 & 0 & X(k,q) & 0 \\ Y(k,q) & 0 & 0 & Z(q) \end{pmatrix}. \end{aligned} \quad (42)$$

Here, the matrix representation is in the basis (32) and the abbreviations

$$X(k,q) = |F(k)|^2 |F(q)|^2, \quad (43)$$

$$Y(k,q) = G(k)G(q) \left[\left(1 + \frac{1}{2} S \right) - |F(k)|^2 - |F(q)|^2 \right], \quad (44)$$

$$Z(k) = X(k,k) + Y(k,k) \quad (45)$$

were introduced, and S is the sum over all expansion coefficients squared,

$$S = \sum_{k'} G^2(k'). \quad (46)$$

The value of S depends on the number of states that are available, i.e., the wave vectors over which the sum runs. The density of states increases with the sample area A and hence the value of S depends on A . In the limit of $A \gg \frac{2\pi}{L} \left(\frac{c}{\omega_{12}} \right)^2$ (see Appendix B), one can take the limit $S \rightarrow \infty$ and obtain

$$\begin{aligned} \rho^a &\stackrel{S \rightarrow \infty}{=} \frac{1}{G^2(k) + G^2(q)} \\ &\times \begin{pmatrix} G^2(k) & 0 & 0 & G(k)G(q) \\ 0 & 0 & 0 & 0 \\ 0 & 0 & 0 & 0 \\ G(k)G(q) & 0 & 0 & G^2(q) \end{pmatrix}. \end{aligned} \quad (47)$$

This corresponds to the pure photon state,

$$|\psi^a\rangle = \frac{1}{\sqrt{G^2(k) + G^2(q)}} (G(k) |\mathbf{k}\rangle_L |\mathbf{k}\rangle_R + G(q) |\mathbf{q}\rangle_L |\mathbf{q}\rangle_R). \quad (48)$$

C. Measure of entanglement

The state ρ^a , which we derived from $|G^{(2)}\rangle$, describes two photons that propagate with opposite in-plane wave vectors in the microcavity and that can potentially be released by an appropriate time modulation (quench) of the Rabi frequency $\Omega_R(k)$. Since one chooses the modes \mathbf{k} and $-\mathbf{k}$ and accordingly \mathbf{q} and $-\mathbf{q}$ via the postselection, the photons effectively form a two-qubit system. For such a system, the entanglement for mixed states can be calculated analytically without evaluating a convex roof explicitly from the density matrix by way of the concurrence $C(\rho)$.⁴⁵ With this function, the so-called entanglement of formation $E_F(\rho)$ (Ref. 43) of two qubits can be easily calculated via⁴⁵

$$E_F(\rho) = h \left(\frac{1 + \sqrt{1 - C^2(\rho)}}{2} \right), \quad (49)$$

with the binary entropy

$$h(x) = -x \log_2(x) - (1-x) \log_2(1-x). \quad (50)$$

The concurrence itself is given by⁴⁵

$$C(\rho) = \max\{0, \lambda_1 - \lambda_2 - \lambda_3 - \lambda_4\}. \quad (51)$$

Here, λ_1 to λ_4 are, in decreasing order, the square roots of the eigenvalues of the matrix $\rho \tilde{\rho}$, and $\tilde{\rho}$ is a transformation of the

density matrix given by⁴⁵

$$\tilde{\rho} = (\sigma_y \otimes \sigma_y) \rho^* (\sigma_y \otimes \sigma_y), \quad (52)$$

where σ_y is the Pauli y matrix and the $*$ denotes complex conjugation.

1. Analytical results

For the photonic state ρ^a (42), the parameters λ_1 to λ_4 are found to be

$$\lambda_1 = \frac{1}{N_{\text{LR}}^2} (\sqrt{Z(k)Z(q)} + Y(k,q)), \quad (53)$$

$$\lambda_2 = \frac{1}{N_{\text{LR}}^2} (\sqrt{Z(k)Z(q)} - Y(k,q)), \quad (54)$$

$$\lambda_{3,4} = \frac{1}{N_{\text{LR}}^2} X(k,q). \quad (55)$$

Hence, from Eq. (51), we obtain in connection with (43)–(45) for the concurrence,

$$\begin{aligned} C(\rho^a) &= C(k,q) \\ &= \frac{2}{N_{\text{LR}}^2} \left\{ G(k)G(q) \left[1 + \frac{1}{2}S - |F(k)|^2 - |F(q)|^2 \right] \right. \\ &\quad \left. - |F(k)|^2 |F(q)|^2 \right\}. \end{aligned} \quad (56)$$

The concurrence thus only depends on the absolute values k and q via the expansion coefficients, which were given in Eqs. (21) and (22),

$$\begin{aligned} G(k) &= \frac{\bar{\omega}_{12}(k) + \omega_c(k) - \omega_{\text{LP}}(k) - \omega_{\text{UP}}(k)}{\bar{\omega}_{12}(k) - \omega_c(k) - \omega_{\text{LP}}(k) - \omega_{\text{UP}}(k)}, \\ |F(k)| &= \frac{\bar{\omega}_{12}(k)}{\Omega_{\text{R}}(k)} G(k). \end{aligned}$$

We have investigated the role of Coulomb interactions [entering via $\bar{\omega}_{12}(k)$] for the concurrence, and found that the Coulomb corrections are on the order of 5% or less for our choice of parameters.⁴⁶ The further numerical analysis of $C(k,q)$ was performed without Coulomb corrections.

To show the dependence of the concurrence on k and q , we have to evaluate the sum S explicitly. Using a sample area $A = (200 \text{ } \mu\text{m})^2$, we find $S = 0.857$. The result is presented in Fig. 6 for the same parameters as used before, where $C(k,q)$ is shown in a density plot as a function of the modes k and q . Below it, we show cuts for different values of q to better illustrate the dependency of the concurrence. One can observe two branches of high entanglement that appear for large values of k and/or q . Their appearance can be explained by the characteristics of the expansion coefficient $G(k)$ for large k . $G(k)$ tends to zero as $1/k^2$, hence $|F(k)|^2$ scales as $1/k^3$. Hence for the diagonal branch, i.e., $k \approx q$, the $|F|$ terms in Eqs. (56) and (A2) can be neglected and we obtain

$$C(k,q) \stackrel{k,q \rightarrow \infty}{\approx} \frac{2G(k)G(q)}{G^2(k) + G^2(q)} \stackrel{k \approx q}{\approx} 1. \quad (57)$$

Accordingly, photons with frequencies in the visible range are almost maximally entangled if their wave numbers are of the same size.

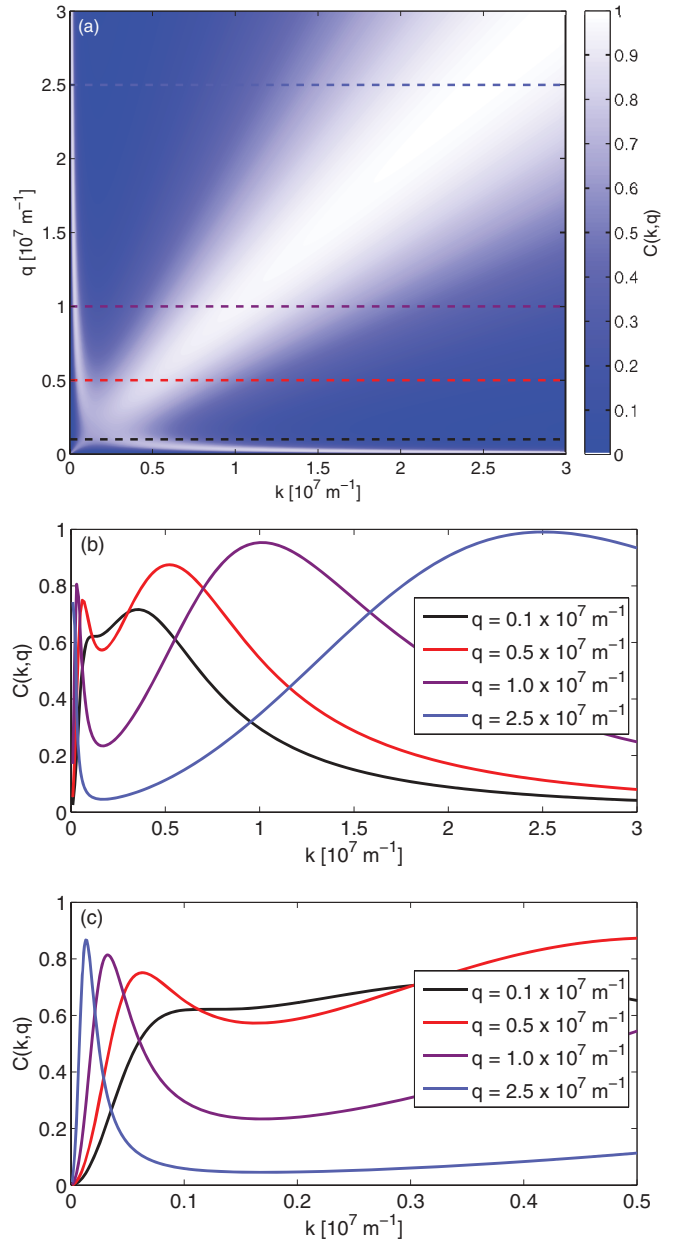


FIG. 6. (Color online) (a) The concurrence $C(k,q)$ as a function of k and q for GaAs/AlGaAs quantum wells. (Parameter values: $\varepsilon = 10$, $m^* = 0.067m_0$, $n_{\text{QW}}^{\text{eff}} = 50$, $L_c^{\text{eff}} = 2 \text{ } \mu\text{m}$, $\hbar\omega_{12} = 113 \text{ meV}$, $N_{2\text{DEG}} = 10^{12} \text{ cm}^{-2}$.) (b) Plot of $C(k,q)$ for fixed values of q (given in the respective legend) and for a large range of k from 0 to $3 \times 10^7 \text{ m}^{-1}$, which corresponds to a photon energy of 1.9 eV (450 THz, red). (c) Zoom in the region only up to $k = 0.5 \times 10^7 \text{ m}^{-1}$ (320 meV, 80 THz, midinfrared).

The other branch appears if $G(k) \approx G(q)$ and the modes are far from each other. We give a more precise analysis of expression (57) in the next section, where the limit of large sample areas is worked out.

In Fig. 7, we present the concurrence for two other values of ω_{12} , namely, $\hbar\omega_{12} = 50 \text{ meV}$ and $\hbar\omega_{12} = 150 \text{ meV}$. Qualitatively, the concurrence shows the two characteristic branches of high entanglement mentioned before for a large range of intersubband energies $\hbar\omega_{12}$. The position of the

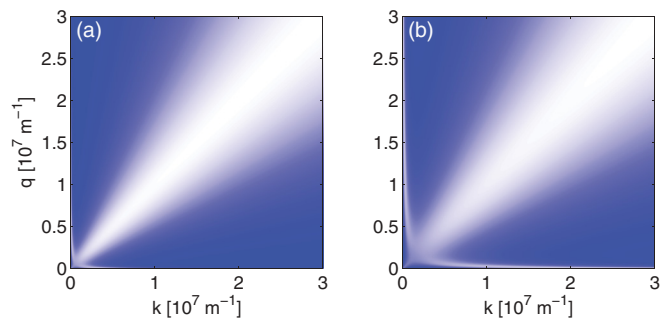


FIG. 7. (Color online) The concurrence $C(k, q)$ for renormalized intersubband transition energies of (a) $\hbar\omega_{12} = 50$ meV and (b) $\hbar\omega_{12} = 150$ meV. [Other parameters have same values as before, besides $L_c^{\text{eff}} = 5 \mu\text{m}$ in (a).] The color scale is identical to that of Fig. 6.

side branch, however, shifts due to changes in the expansion coefficient $G(k)$.

2. Large-cavity limit

The case of a large cavity, i.e., a large sample area A , is described by the limit $S \rightarrow \infty$; see Appendix B. The concurrence in this case is calculated to be

$$C(k, q) = \frac{2G(k)G(q)}{G^2(k) + G^2(q)}. \quad (58)$$

In this limit, the sample area A drops out so that $C(k, q)$ becomes independent of A . We show the result in Fig. 8. As one can see, the concurrence always has two maxima if q is held constant. One maximum appears for $G(k) = G(q)$ and $k \neq q$.

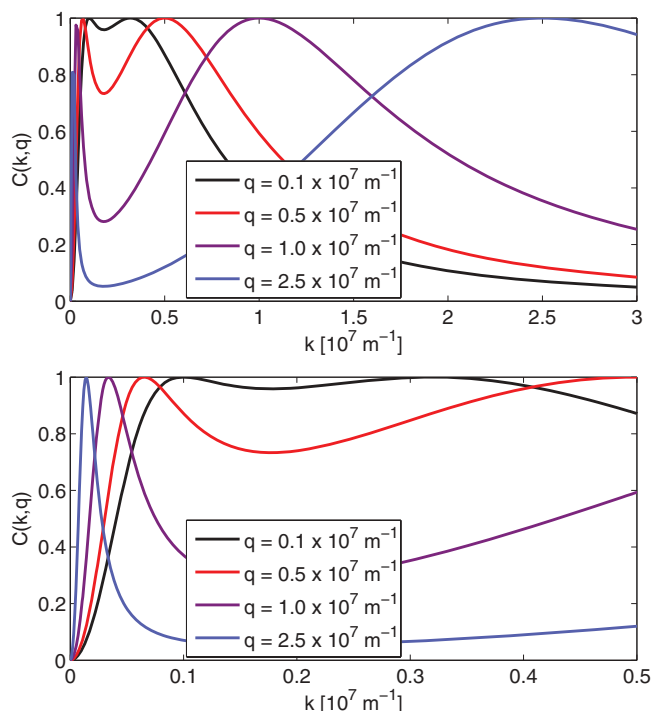


FIG. 8. (Color online) The concurrence $C(k, q)$ in the case of large sample areas for GaAs/AlGaAs quantum wells. (Parameter values: $\varepsilon = 10$, $m^* = 0.067m_0$, $n_{\text{QW}}^{\text{eff}} = 50$, $L_c^{\text{eff}} = 2 \mu\text{m}$, $\hbar\omega_{12} = 113$ meV, $N_{2\text{DEG}} = 10^{12} \text{cm}^{-2}$.)

There, photons are maximally entangled since we have $C = 1$. However, this maximum is relatively sharply peaked and if one realizes the postselection experimentally by choosing a certain finite k range, then the entanglement will be reduced. The other maximum appears when $k = q$, which seems to be an artifact of the calculation, since this specific point was excluded in the calculations above. The reason for the exclusion is that the two-photon states would be separable and hence not entangled. However, all of the states with $k \approx q$ in the vicinity of this point are allowed by the postselection. Therefore, one can see from the broad shape of this second maximum that for a given q , there exists a wide range of corresponding modes k , for which the two photons are almost maximally entangled. The only request for k and q is that the difference between them can be resolved experimentally. In the second plot of Fig. 8, we show a magnification for wave vectors up to $0.5 \times 10^7 \text{m}^{-1}$ to more clearly show the dependence of $C(k, q)$ on k around the first maximum, which is not visible in the previous plot. Particularly at the intersubband resonance, which is around $0.1 \times 10^7 \text{m}^{-1}$, the two maxima approach each other so that by selecting different modes around the resonance, the entanglement of the photons can be made almost maximal. The corresponding photon energies are in the midinfrared regime, about 100–150 meV.

V. CONCLUSION

An efficient and deterministic source of entangled photons is needed in quantum information processing. In this work, we examined a scheme of entangled photon production, based on the emission of quantum vacuum radiation from the intersubband cavity system. Because the triggered photon emission is based on a nonadiabatic modulation of the system's ground state, an exact expression for this state could be used. Since the ground state consists of an infinite number of photonic and electronic states, we propose a postselective measurement to reduce the photonic system to an effective two-qubit system, in which the qubit state was defined as two different in-plane wave vectors. The so-called mode entanglement of the photons is quantified by the concurrence. We found an analytical expression for the concurrence, which depends on the absolute values of the chosen wave vectors. We found that the concurrence, and therefore the entanglement of the postselected photons, is nonzero. In the limiting case of large sample areas, there exists a continuous set of mode pairs for which the concurrence is 1, i.e., the photons are maximally entangled. Also, in this case, it turns out that for photon energies around the intersubband resonance, which is in the midinfrared regime of the electromagnetic spectrum, the photons are almost maximally entangled, with the concurrence being close to 1. This is fundamentally important for the possible use in quantum information processing. Furthermore, a high degree of entanglement can be achieved if the modes chosen in the postselection are close to each other. Therefore, one could extract entangled photon pairs in technologically relevant frequency domains, such as one of the telecommunication wavelengths.

We also note the possibility of triggering the photon-pair emission by a systematic quench of the light-matter interaction in the microcavity. The repetition rate for the photon

production is limited by the switching times, which have to be fast enough to perturb the system nonadiabatically. The experiments to date have achieved switch-on times of the ultrastrong-coupling regime of about 10 fs (Refs. 16, 37, and 38) by ultrashort laser pulses. The switch-off, which is the important operation related to photon emission, has to be as fast as this time scale, which gives a rough estimate for the repetition rate of 10^{13} – 10^{14} full cycles (switch-on and switch-off) per second. The probability then to really measure a desired two-photon state is given by the probability of a successful postselection.

Further work is required to model noninstantaneous switch-off processes, presumably using a time-dependent perturbation-theory approach. Another open issue is the simultaneous emission of blackbody radiation at finite temperature,

an effect which is expected to be small compared to the vacuum radiation,³⁶ but which will to some extent reduce the average entanglement of the emitted photons.

ACKNOWLEDGMENTS

The authors thank A. Pashkin and R. Huber for useful discussions and acknowledge funding from the DFG within SFB 767.

APPENDIX A: POSTSELECTED STATE

The pure state $|\psi_{\text{LR}}\rangle$, which contains all two-photon states fulfilling the conditions of the postselection, is given as

$$\begin{aligned} |\psi_{\text{LR}}\rangle &= \frac{\tilde{N}}{N_{\text{LR}}} \mathcal{P}_{\text{LR}} |G^{(2)}\rangle \\ &= \frac{1}{N_{\text{LR}}} \left[(G(k)|\mathbf{k}\rangle_{\text{L}}|\mathbf{k}\rangle_{\text{R}} + G(q)|\mathbf{q}\rangle_{\text{L}}|\mathbf{q}\rangle_{\text{R}}) \otimes \left(|0\rangle_b + \frac{1}{2} \sum_{k'} G(k') b_{k'}^\dagger b_{-k'}^\dagger |0\rangle_b \right) + F^2(k)|\mathbf{k}\rangle_{\text{L}}|\mathbf{k}\rangle_{\text{R}} \otimes b_{-k}^\dagger b_k^\dagger |0\rangle_b \right. \\ &\quad \left. + F^2(q)|\mathbf{q}\rangle_{\text{L}}|\mathbf{q}\rangle_{\text{R}} \otimes b_{-q}^\dagger b_q^\dagger |0\rangle_b + F(k)F(q)|\mathbf{q}\rangle_{\text{L}}|\mathbf{k}\rangle_{\text{R}} \otimes b_{-k}^\dagger b_q^\dagger |0\rangle_b + F(k)F(q)|\mathbf{k}\rangle_{\text{L}}|\mathbf{q}\rangle_{\text{R}} \otimes b_{-q}^\dagger b_k^\dagger |0\rangle_b \right], \end{aligned} \quad (\text{A1})$$

with N_{LR} being a normalization constant,

$$\begin{aligned} N_{\text{LR}}^2 &= [G^2(k) + G^2(q)] \left(1 + \frac{1}{2} S \right) + [|F(k)|^2 + |F(q)|^2]^2 \\ &\quad - 2G^2(k)|F(k)|^2 - 2G^2(q)|F(q)|^2. \end{aligned} \quad (\text{A2})$$

We already introduced the sum S as being

$$S = \sum_{k'} G^2(k'). \quad (\text{A3})$$

APPENDIX B: CONTINUUM LIMIT

When taking the sum over all two-dimensional in-plane wave vectors \mathbf{k} in Eq. (46), the appearing vectors depend on the boundary conditions. We choose periodic boundary conditions, and hence

$$k_x = \frac{2\pi}{L_x} n_x, \quad n_x = 0, \pm 1, \dots, \quad (\text{B1})$$

$$k_y = \frac{2\pi}{L_y} n_y, \quad n_y = 0, \pm 1, \dots, \quad (\text{B2})$$

where $L_{x(y)}$ is the cavity length in the $x(y)$ direction and $n_{x(y)}$ is an integer. Every discrete wave vector \mathbf{k} has a volume Δ in \mathbf{k} space:

$$\Delta = \Delta k_x \Delta k_y = \frac{(2\pi)^2}{L_x L_y} = \frac{(2\pi)^2}{A}, \quad (\text{B3})$$

and $\Delta k_{x(y)}$ is the difference between two adjacent wave vectors in the $x(y)$ direction, where A is the sample area. In the continuum limit, the \mathbf{k} vectors lie close in the reciprocal space

and the sum can be replaced by an integral,

$$\begin{aligned} S &= \sum_{\mathbf{k}} G^2(k) = \frac{1}{\Delta} \sum_{\mathbf{k}} \Delta G^2(k) \rightarrow \frac{1}{\Delta} \int d^2k G^2(k) \\ &= \frac{A}{2\pi} \int_{k=0}^{\infty} dk k G^2(k) = \frac{A}{2\pi} \left(\frac{\omega_{12}}{c} \right)^2 \mathcal{I}, \end{aligned} \quad (\text{B4})$$

where we use polar coordinates to evaluate the integral and carry out the polar-angle integration. In the last step, we make a substitution and introduce the dimensionless variable $\tilde{k} := \frac{c}{\omega_{12}} k$ to get the dimensionless integral \mathcal{I} ,

$$\mathcal{I} = \int_{\tilde{k}=0}^{\infty} d\tilde{k} \tilde{k} G^2\left(\frac{c}{\omega_{12}} \tilde{k}\right). \quad (\text{B5})$$

One can show that the expansion coefficient $G(k)$ decreases like $1/k^2$ for large k . Consequently, the integrand has the asymptotics

$$k G^2(k) \stackrel{k \rightarrow \infty}{\approx} \frac{1}{k^3}, \quad (\text{B6})$$

and hence the integral converges. We evaluate \mathcal{I} numerically using the same parameters as above and find $\mathcal{I} = 4.1 \times 10^{-4}$.

*adrian.auer@uni-konstanz.de

- ¹M. A. Nielsen and I. L. Chuang, *Quantum Computation and Quantum Information* (Cambridge University Press, Cambridge, 2000).
- ²A. Einstein, B. Podolsky, and N. Rosen, *Phys. Rev.* **47**, 777 (1935).
- ³E. Schrödinger, *Naturwissenschaften* **23**, 807 (1935).
- ⁴A. K. Ekert, *Phys. Rev. Lett.* **67**, 661 (1991).
- ⁵C. H. Bennett, G. Brassard, C. Crépeau, R. Jozsa, A. Peres, and W. K. Wootters, *Phys. Rev. Lett.* **70**, 1895 (1993).
- ⁶C. H. Bennett and S. J. Wiesner, *Phys. Rev. Lett.* **69**, 2881 (1992).
- ⁷H.-J. Briegel, W. Dür, J. I. Cirac, and P. Zoller, *Phys. Rev. Lett.* **81**, 5932 (1998).
- ⁸P. G. Kwiat, K. Mattle, H. Weinfurter, A. Zeilinger, A. V. Sergienko, and Y. Shih, *Phys. Rev. Lett.* **75**, 4337 (1995).
- ⁹O. Benson, C. Santori, M. Pelton, and Y. Yamamoto, *Phys. Rev. Lett.* **84**, 2513 (2000).
- ¹⁰C. Ciuti, G. Bastard, and I. Carusotto, *Phys. Rev. B* **72**, 115303 (2005).
- ¹¹*Intersubband Transitions in Quantum Wells: Physics and Device Applications I*, edited by H. C. Liu and F. Capasso, Semiconductors and Semimetals Vol. 62 (Academic Press, San Diego, 2000).
- ¹²*Intersubband Transitions in Quantum Wells: Physics and Device Applications II*, edited by H. C. Liu and F. Capasso, Semiconductors and Semimetals Vol. 66 (Academic Press, San Diego, 2000).
- ¹³J. Faist, F. Capasso, D. L. Sivco, C. Sirtori, A. L. Hutchinson, and A. Y. Cho, *Science* **264**, 553 (1994).
- ¹⁴R. Köhler, A. Tredicucci, F. Beltram, H. E. Beere, E. H. Linfield, A. G. Davies, D. A. Ritchie, R. C. Iotti, and F. Rossi, *Nature (London)* **417**, 156 (2002).
- ¹⁵R. Colombelli, K. Srinivasan, M. Troccoli, O. Painter, C. F. Gmachl, D. M. Tennant, A. M. Sergent, D. L. Sivco, A. Y. Cho, and F. Capasso, *Science* **302**, 1374 (2003).
- ¹⁶G. Günter, A. A. Anappara, J. Hees, A. Sell, G. Biasiol, L. Sorba, S. De Liberato, C. Ciuti, A. Tredicucci, A. Leitenstorfer, and R. Huber, *Nature (London)* **458**, 178 (2009).
- ¹⁷A. A. Anappara, S. De Liberato, A. Tredicucci, C. Ciuti, G. Biasiol, L. Sorba, and F. Beltram, *Phys. Rev. B* **79**, 201303(R) (2009).
- ¹⁸Y. Todorov, A. M. Andrews, R. Colombelli, S. De Liberato, C. Ciuti, P. Klang, G. Strasser, and C. Sirtori, *Phys. Rev. Lett.* **105**, 196402 (2010).
- ¹⁹M. Geiser, F. Castellano, G. Scalari, M. Beck, L. Nevou, and J. Faist, *Phys. Rev. Lett.* **108**, 106402 (2012).
- ²⁰J. Bourassa, J. M. Gambetta, A. A. Abdumalikov Jr., O. Astafiev, Y. Nakamura, and A. Blais, *Phys. Rev. A* **80**, 032109 (2009).
- ²¹T. Niemczyk, F. Deppe, H. Huebl, E. P. Menzel, F. Hocke, M. J. Schwarz, J. J. Garcia-Ripoll, D. Zueco, T. Hümmer, E. Solano, A. Marx, and R. Gross, *Nature Phys.* **6**, 772 (2010).
- ²²P. Forn-Díaz, J. Lisenfeld, D. Marcos, J. J. García-Ripoll, E. Solano, C. J. P. M. Harmans, and J. E. Mooij, *Phys. Rev. Lett.* **105**, 237001 (2010).
- ²³C. M. Wilson, G. Johansson, A. Pourkabirian, M. Simoen, J. R. Johansson, T. Duty, F. Nori, and P. Delsing, *Nature (London)* **479**, 376 (2011).
- ²⁴W. Vogel and D.-G. Welsh, *Quantum Optics* (Wiley-VCH, Weinheim, Germany, 2006).
- ²⁵D. E. Nikonov, A. Imamoğlu, L. V. Butov, and H. Schmidt, *Phys. Rev. Lett.* **79**, 4633 (1997).
- ²⁶S. De Liberato and C. Ciuti, *Phys. Rev. B* **85**, 125302 (2012).
- ²⁷Y. Todorov and C. Sirtori, *Phys. Rev. B* **85**, 045304 (2012).
- ²⁸S. De Liberato and C. Ciuti, *Phys. Rev. Lett.* **102**, 136403 (2009).
- ²⁹D. Hagenmüller, S. De Liberato, and C. Ciuti, *Phys. Rev. B* **81**, 235303 (2010).
- ³⁰J. J. Hopfield, *Phys. Rev.* **112**, 1555 (1958).
- ³¹A. Quattropani, L. C. Andreani, and F. Bassani, *Nuovo Cimento D* **7**, 55 (1986).
- ³²D. Dini, R. Köhler, A. Tredicucci, G. Biasiol, and L. Sorba, *Phys. Rev. Lett.* **90**, 116401 (2003).
- ³³A. A. Anappara, A. Tredicucci, G. Biasiol, and L. Sorba, *Appl. Phys. Lett.* **87**, 051105 (2005).
- ³⁴A. A. Anappara, A. Tredicucci, F. Beltram, G. Biasiol, and L. Sorba, *Appl. Phys. Lett.* **89**, 171109 (2006).
- ³⁵C. Ciuti and I. Carusotto, *Phys. Rev. A* **74**, 033811 (2006).
- ³⁶S. De Liberato, C. Ciuti, and I. Carusotto, *Phys. Rev. Lett.* **98**, 103602 (2007).
- ³⁷R. Huber, A. A. Anappara, G. Günter, A. Sell, S. De Liberato, C. Ciuti, G. Biasiol, L. Sorba, A. Tredicucci, and A. Leitenstorfer, *J. Appl. Phys.* **109**, 102418 (2011).
- ³⁸M. Porer, J.-M. Ménard, A. Leitenstorfer, R. Huber, R. Degl'Innocenti, S. Zanatto, G. Biasiol, L. Sorba, and A. Tredicucci, *Phys. Rev. B* **85**, 081302(R) (2012).
- ³⁹A. Ridolfo, R. Vilardi, O. Di Stefano, S. Portolan, and S. Savasta, *Phys. Rev. Lett.* **106**, 013601 (2011).
- ⁴⁰R. Horodecki, P. Horodecki, M. Horodecki, and K. Horodecki, *Rev. Mod. Phys.* **81**, 865 (2009).
- ⁴¹D. Bouwmeester, A. K. Ekert, and A. Zeilinger, *The Physics of Quantum Information: Quantum Cryptography, Quantum Teleportation, Quantum Computation* (Springer, New York, 2001).
- ⁴²M. B. Plenio and S. Virmani, *Quantum Inf. Comput.* **7**, 1 (2007).
- ⁴³C. H. Bennett, D. P. DiVincenzo, J. A. Smolin, and W. K. Wootters, *Phys. Rev. A* **54**, 3824 (1996).
- ⁴⁴S. Hill and W. K. Wootters, *Phys. Rev. Lett.* **78**, 5022 (1997).
- ⁴⁵W. K. Wootters, *Phys. Rev. Lett.* **80**, 2245 (1998).
- ⁴⁶For our choice of parameters, the depolarization shift $\delta(k)$ is less than 10%. Expanding the concurrence $\bar{C}(k, q)$ including Coulomb interactions to the first order in $\delta(k)$ leads us to $\bar{C}(k, q) \approx C(k, q)[1 + \delta(k)\alpha(k, q) + \delta(q)\alpha(q, k)]$ with $\delta(k)\alpha(k, q) + \delta(q)\alpha(q, k) < 0.05$, where $\alpha(k, q)$ is an expansion coefficient.